Orographic Influences on Subtropical Stratocumulus

I. RICHTER AND C. R. MECHOSO

Department of Atmospheric and Oceanic Sciences, University of California, Los Angeles, Los Angeles, California

(Manuscript received 15 June 2005, in final form 6 January 2006)

ABSTRACT

The impact of South American orography on subtropical stratocumulus clouds off the Peruvian coast is investigated in the context of an atmospheric general circulation model. It is found that stratocumulus incidence is significantly reduced when South American orography is removed. Key to this behavior is a decrease in lower tropospheric stability (LTS) that allows for more frequent stratocumulus destruction through the model's cloud-top entrainment instability mechanism. The role of orography in enhancing Peruvian stratocumulus is as follows. Within the PBL, orography deflects the midlatitude westerly winds equatorward in association with cold air advection and blocking of the low-level flow from the continent. Above the PBL, the steep and high South American orography deflects a significant portion of the midlatitude westerlies equatorward. This flow sinks along the equatorward sloping isentropes, thus promoting subsidence. Both processes increase LTS over the stratocumulus region. In further AGCM experiments, the sensitivity of Peruvian stratocumulus to the use of unsmoothed orographic boundary conditions is assessed. The results show no significant differences to the control simulation, which uses smoothed orography. This suggests that, in the context of GCMs, a representation of South American orography more detailed than is generally used has little potential for improving the performance of coupled ocean–atmosphere models in the eastern tropical Pacific.

1. Introduction

The importance of stratocumulus to the climate system has been recognized for a long time. Their high reflectivity and low cloud-base height imply net cooling of the underlying surface. Particularly over the oceans, where stratocumulus decks often provide persistent cloud cover over vast areas, their radiative impact is significant and plays a vital role in regulating surface temperatures. This is evident in the eastern subtropical oceans, where persistent cloud decks are accompanied by sea surface temperatures (SSTs) that are much colder than the zonal mean. Any attempt to model realistically the tropical or global climate system is therefore dependent on the successful simulation of stratocumulus. Such a requirement poses a particularly challenging problem in the context of large-scale climate models, which cannot explicitly resolve turbulent processes within the planetary boundary layer (PBL) and its interface with the free troposphere.

Underprediction of stratocumulus in models of the coupled ocean–atmosphere system typically leads to a warm bias in underlying sea surface temperatures (SSTs) with severe drifts in the simulated climate (Mechoso et al. 1995; Davey et al. 2002). To the present day, difficulties in simulating stratocumulus remain a major source of error in climate simulations and contribute significantly to the uncertainties in the prediction of global warming. An improved understanding of stratocumulus and their interaction with the large-scale environment is needed to guide efforts toward a more successful representation of cloud–radiation interactions in large-scale climate models.

The processes that generate and dissipate stratocumulus have been the subject of intense research efforts and much progress has been made during the last few decades in identifying and describing the relevant phenomena. Nevertheless, many aspects are still rather poorly understood. Chief among those are the entrainment process at cloud top (e.g., Stevens 2002) and the conditions under which stratocumulus become unstable (e.g., Bretherton and Wyant 1997). Apart from these

Corresponding author address: Ingo Richter, University of California, Los Angeles, Dept. of Atmospheric and Oceanic Sciences, 7127 Math Sciences Building, 405 Hilgard Ave., Los Angeles, CA 90095.
E-mail: richter@atmos.ucla.edu

local considerations there is also the question as to how the general circulation partakes in the maintenance and destruction of stratocumulus. With respect to the eastern subtropical oceans, it has been established that large-scale subsidence and associated warming above the PBL contribute to lower tropospheric stability[1] (LTS), thereby providing an environment conducive to the persistence of stratocumulus. Subsidence in those regions may be modulated by the strength of the Hadley circulation as well as convection over adjacent continents. Surface winds associated with the eastern branches of the marine subtropical anticyclones also contribute in two ways. First, they provide cold air advection into the stratocumulus regions at lower latitudes. Second, their alongshore component induces coastal upwelling with its associated cooling effect on SSTs, which in turn increases LTS.

Three regions of particularly persistent and expansive marine stratocumulus decks are located to the west of California, Peru/Chile, and Namibia/Angola. Common to all these regions is their proximity to substantial orography on the adjacent continents. It is well known that orography has a profound impact on the general circulation (e.g., Charney and Eliassen 1949; Held and Ting 1990; Ringler and Cook 1999). This raises the question whether orography also contributes to the behavior of stratocumulus to the west of continental landmasses. A recent study by Xu et al. (2004) found that removal of the Andes Mountains in a regional climate model significantly reduced incidence of stratocumulus off the Peruvian coast. Xu et al. attributed this result to the intrusion of dry warm air from the South American continent that can occur within the PBL when the orographic barrier between ocean and land is removed. Richter and Mechoso (2004) found a similar impact of African orography on Namibian stratocumulus in a sensitivity study with a general circulation model (GCM). However, they also found a similarly strong impact from local circulation changes *above* the PBL. For example, temperatures at 700 mb and thus LTS over the Namibian stratocumulus region were significantly reduced when orography was removed. Prominent in their results was an anticyclonic circulation pattern centered over the orography of southern Africa that gave way to a more zonal flow in the absence of orography. The orographically induced anticyclonic circulation was found to advect warm air poleward on its Atlantic flank and thus contribute to temperatures warmer than the zonal mean and a high value of LTS.

South American orography is too high and steep to permit an anticyclonic circulation similar to the one seen over southern Africa. Nevertheless, the eastern tropical Pacific also features temperatures in the lower troposphere that are significantly higher than the zonal mean. Thus, if South American orography contributes to these warm temperatures, it must do so by different means than its African counterpart. In the present study we will address if and how South American orography influences lower tropospheric temperatures to the west and how this relates to the behavior of stratocumulus.

Apart from the fundamental question of how subtropical stratocumulus is affected by the removal of orography, there is the question whether different representations of orography may also alter the incidence of stratocumulus in the context of a GCM. Many GCMs (including the one used in this study) use orographic boundary conditions with some degree of smoothing in order to avoid computational problems associated with the pressure gradient force error in sigma coordinates near steep orography (Mellor et al. 1994; Webster et al. 2003). Owing to their steepness the Andes are generally subjected to this kind of treatment. In the case of the GCM used in this study, smoothing reduces the height of the Andes by about 1000 m, resulting in peak heights of about 3000 m. Xu et al. (2004) suggest that such underrepresentation of the Andes can result in a significant decrease in the incidence of simulated Peruvian stratocumulus. Their results were obtained by replacing the high-resolution orography in a regional model with a smoothed GCM orography. One can ask whether the opposite result can be obtained by using an unsmoothed orography in the context of a GCM.

In summary, we address the following three issues in this paper: 1) How does the removal of South American orography influence Peruvian stratocumulus? 2) How does the impact differ from what Richter and Mechoso (2004) found in the case of southern Africa? 3) Does smoothing of the Andes deteriorate the simulation of Peruvian stratocumulus?

Our approach to addressing the above issues is based on numerical simulations with an atmospheric GCM (AGCM). Idealized studies with modified orographic boundary conditions can be undertaken without difficulty in such a model. The particular model used in this study is the University of California, Los Angeles (UCLA) AGCM. One unique aspect of the UCLA AGCM is its treatment of the PBL top as a coordinate surface. This facilitates the parameterization of PBL clouds and frees the model from explicitly modeling the sharp temperature and moisture jumps that typically occur across the PBL top. As a result, the UCLA

[1] LTS can be defined, for example, as the difference in potential temperature between 700 mb and the surface.

AGCM achieves a realistic simulation of stratocumulus in terms of their seasonal cycle and geographical distribution.

Addressing the impact of orography in the context of an AGCM with SST provided by an observed climatology allows for a clean comparison between results. We recognize, however, that the procedure is not free of inconsistencies as it does not consider the SST response to atmospheric circulation changes in the absence of mountains. Kitoh (2002, 2004) has recently addressed the impact of orography on earth's climate with a coupled ocean–atmosphere model. In his experiments, the complete removal of the global orography led to a weakening of the anticyclone over the subtropical Pacific accompanied by reduced low-level cloud and increased SST to the northeast. The author interprets these features as part of the Rossby wave response to the weakening of the Asian and North American summer monsoons, which results from elimination of the elevated heat source and orographic uplift. Idealized studies by Hoskins (1996) and Rodwell and Hoskins (2001) give support to this idea.

Kitoh (2002, 2004) found a qualitatively similar response to orography in the southeast Atlantic and Pacific, but his analysis focuses on the Northern Hemisphere and does not address this feature in detail. The intensification of subtropical highs induced by Rossby wave propagation originated through convection on the continents, however, may be of less relevance to the southeast Pacific where stratocumulus incidence does not peak in the warm season.

Kitoh (2004) also addressed the importance of oceanic feedbacks by performing no-mountain experiments with both an AGCM and a coupled ocean–atmosphere GCM. His results show that coupled feedbacks in the subtropical regions intensify the orographic effect but do not change it qualitatively. This suggests that our AGCM-based approach will be able to capture the essence of the circulation changes accompanying the removal of orography, even though coupled feedbacks are not included. Therefore, the experiments presented in this study provide a stepping stone toward a better understanding of the orographic influence on stratocumulus. A reexamination within the framework of a coupled ocean–atmosphere system will be required to properly assess the importance of coupled feedbacks.

The paper is organized as follows. Section 2 briefly describes the UCLA AGCM and the setup of the sensitivity experiments. In section 3a we analyze circulation changes above and inside the PBL that result from removing South American orography. Section 4 contrasts the results from section 3 with the African case. In section 5 we address the impact that smoothing might have on the simulation of Peruvian stratocumulus. In section 6 we summarize and discuss our results. Conclusions are given in section 7.

2. Model description and experiment design

The UCLA AGCM solves the primitive equations on a sphere using the Arakawa C grid for horizontal discretization. The model's vertical coordinate is the modified σ coordinate, described in Suarez et al. (1983), in which the PBL is represented by the lowest model layer. The model's prognostic variables are horizontal velocity, potential temperature, surface pressure, PBL depth, water vapor mixing ratio, cloud water mixing ratio, cloud ice mixing ratio, ground temperature, and snow depth over land. Details on the differencing schemes and other aspects of the model can be found online at http://www.atmos.ucla.edu/~mechoso/esm/agcm.html.

The parameterization of cumulus convection in the UCLA AGCM is a version of the Arakawa–Schubert scheme (Arakawa and Schubert 1974) in which the cloud work function quasi equilibrium is relaxed by predicting the cloud-scale kinetic energy (Pan and Randall 1998) and that includes the effects of convective downdrafts (Cheng and Arakawa 1997). Shortwave and longwave radiation are parameterized following Harshvardhan et al. (1987, 1989). Cloud liquid water and ice are predicted based on a five-phase bulk microphysics scheme (Köhler 1999).

The PBL parameterization, presented in Suarez et al. (1983), is based on the mixed-layer framework of Lilly (1968). Parameterization of surface fluxes closely follows the bulk formulae proposed by Deardorff (1972). This formulation relates the turbulence surface fluxes of momentum, latent heat and sensible heat to the bulk mean properties of the PBL, ground temperature, and PBL depth. Modifications by Li et al. (1999, 2002) have significantly improved the simulation of PBL clouds and surface fluxes of radiation and latent heat.

The PBL is assumed to be well mixed with respect to potential temperature and water vapor mixing ratio. If, based on these neutral profiles, saturation occurs below the PBL top, a cloudy sublayer is diagnosed and its properties are passed to the radiation scheme. In the case of saturation, the PBL is no longer well-mixed with regard to potential temperature and the layer mean potential temperature has to be reinterpreted as representing the subcloud layer only. Accordingly, the slope of the in situ temperature profile will change in the PBL, and, based on the liquid water mixing ratio at

PBL top, a new value for PBL-top temperature has to be calculated.

The parameterization of the entrainment rate (E) at PBL top is described in Suarez et al. (1983). Under the assumption that the temporal change of turbulence kinetic energy (TKE) can be neglected, Suarez et al. (1983) write the following relationship:

$$Ee_M = S + B - \rho_M \sigma^3 \tag{1}$$

where e_M is layer mean TKE and S and B are generation of TKE by shear and buoyancy, respectively, ρ_M is the layer mean density, and σ is the dissipation velocity scale of TKE. Expressing all terms on the right-hand side of (1) as a function of E provides an implicit relation for this quantity. More details on the entrainment parameterization used in the UCLA AGCM can be found in Suarez et al. (1983) and Randall (1980a).

It has long been hypothesized that stratocumulus may become unstable depending on the properties of air entrained at cloud top (Lilly 1968). If sufficiently dry and cool, the entrained air can become negatively buoyant, leading to the rapid destruction of the cloud layer. This process has been termed cloud-top entrainment instability (CTEI), and Lilly (1968) formulated a criterion that determines when the process can lead to the destruction of stratocumulus. Randall (1980b) refined Lilly's original criterion by incorporating the effect of liquid water on buoyancy. Accordingly, PBL clouds are destroyed if the following condition is met:

$$\beta \Delta h - \varepsilon \Delta r < 0, \tag{2}$$

where

$$\beta \equiv \frac{1 + 1.608\gamma\varepsilon}{1 + \gamma}, \tag{3}$$

$$\varepsilon \equiv c_p \frac{T}{L}, \tag{4}$$

and

$$\gamma \equiv \frac{L}{c_p}\left(\frac{\partial q^*}{\partial T}\right)_p. \tag{5}$$

In these expressions, h is moist static energy, r is total water mixing ratio, T is temperature, L is the latent heat of condensation, c_p is the specific heat of dry air at constant pressure, q^* is the saturation value of water vapor mixing ratio, and Δ denotes the difference between the PBL and the layer above it (i.e., the lowest two model layers). If (2) is satisfied, mass from the layer above is added to the PBL until either the PBL becomes stable to entrainment or the cloud layer is destroyed, whichever occurs first.

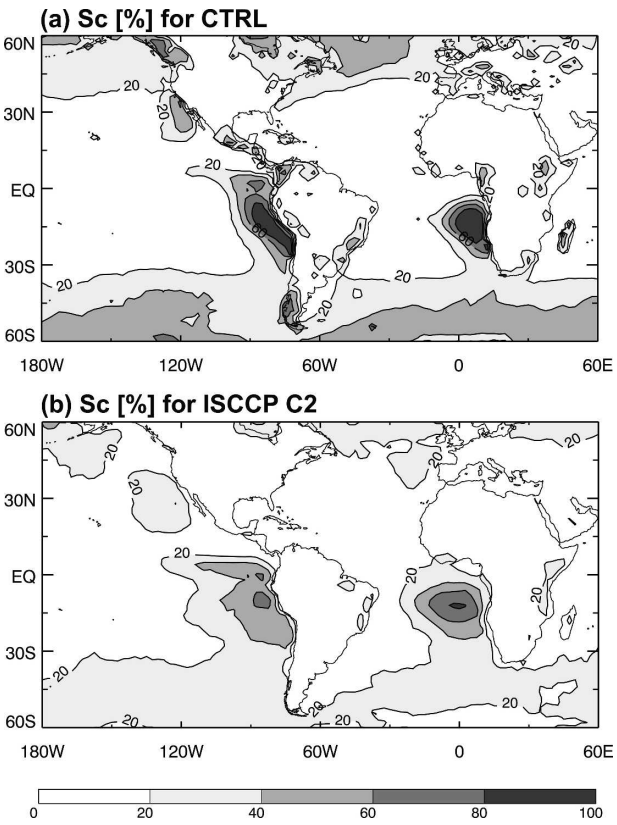

FIG. 1. Stratocumulus incidence in October for (a) CTRL and (b) the ISCCP C2 satellite-derived dataset.

Observational studies in the 1990s and 2000s have not verified the fundamental importance of CTEI to the behavior of stratocumulus on short time scales (e.g., Stevens et al. 2003). The results that we will show in section 3, however, demonstrate that on time scales of several days or longer, application of the CTEI mechanism in the UCLA AGCM establishes a correlation between stratocumulus and LTS that closely resembles observations (Klein and Hartmann 1993; Klein et al. 1995). We interpret this feature in the following way. First, the inequality (2) can be approximated by another on LTS. Second, although (2) for a single grid point and a single time step is only a condition on the sign of the left-hand side, one can assume a posteriori that averaged over many grid points and time steps, larger values of that expression would correspond to a lower incidence of CTEI and vice versa. Thus the left-hand side of (2) is positively correlated with LTS, as presented by Klein and Hartmann (1993), and negatively correlated with CTEI. For ease of reference, we will refer to this quantity as layer cloud stability (LCS).

To illustrate the model's performance in the simulation of stratocumulus clouds, Fig. 1 contrasts simulated

incidence in October (when incidence is maximum along the Peruvian coast, see Fig. 2) with data from the International Satellite Cloud Climatology Project (ISCCP: Rossow and Schiffer 1991). The ISCCP data shown corresponds to a climatological average over eight Octobers from the period 1983–90, while the model results are from a 20-yr control simulation with prescribed climatological SSTs. The model captures the geographical patterns of stratocumulus incidence quite well, with high incidence in the southeast tropical Pacific and Atlantic. Even more subtle features of the observed patterns, such as the westward protrusion of stratocumulus over the eastern equatorial Pacific, are reproduced in the model. The most obvious shortcoming of the model in reference to the ISCCP data is its overprediction of stratocumulus in the southeast Pacific and Atlantic.

The annual cycle of stratocumulus off the coast of Peru is shown in Fig. 2a. The seasonal evolution of cloud incidence is well captured in the model, but values are too low in austral summer and fall. One reason for this feature is that the ISSCP data refers to all cloud below 700 mb, while stratocumulus incidence in our model refers to cloud below the PBL top, which is typically much lower than 700 mb. During austral summer and fall there is considerable cloud cover above the PBL in our model, which, if included in Fig. 2a, would make our results more similar to observations.

Liquid water path (LWP) tends to be overpredicted in the model. In the southeast Pacific, the annual mean of LWP is around 0.015 mm, while satellite observations from the Tropical Rainfall Measuring Mission (TRMM) suggest a typical value of 0.08 mm (see Xu et al. 2004, their Fig. 1a). This overprediction is partially compensated for in the calculation of cloud optical depth (COD; Li et al. 2002), so the simulated radiative impact of stratocumulus is reasonably realistic. More details on the calculation of COD and the model's performance with regard to it can be found in Li et al. (2002).

To investigate the influence of South American orography on Peruvian stratocumulus we perform two AGCM simulations: Control (CTRL hereafter) and No-South-American-Orography (NSAO hereafter) in which South American elevations are set to sea level in the model's boundary conditions. (In the latter simulation, mass was added to the tropospheric model layers in order to have the same global average of sea level pressure as in CTRL.) A third experiment employing unsmoothed South American orography was performed in order to assess the extent to which Peruvian stratocumulus are sensitive to the smoothing of South American orography. This experiment will be referred to as USAO hereafter.

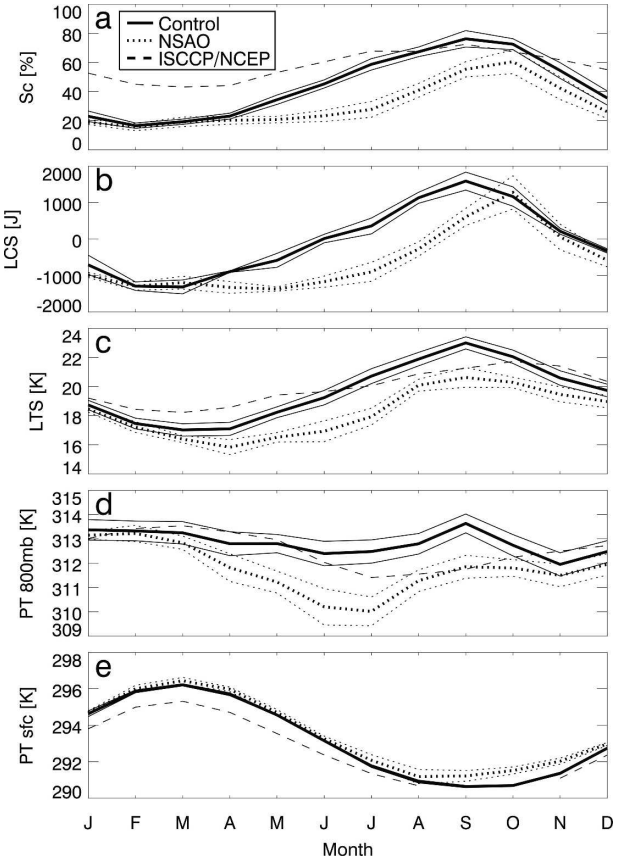

FIG. 2. Annual cycle of (a) stratocumulus incidence (%), (b) moist static energy difference between the lowest two model layers, (c) lower tropospheric stability (K), (d) potential temperature at 700 mb (K), and (e) potential temperature at the surface (K). All terms are area averaged over the Peruvian stratocumulus region as described in the text. The thick solid and dotted lines denote values in CTRL and NSAO. The thin lines show the corresponding standard deviations for individual months. Dashed lines show ISCCP low-level cloudiness in (a), and NCEP reanalysis in (c), (d), and (e).

After a 3-month adjustment period, CTRL, NSAO, and USAO were run for 20, 10, and 5 years, respectively. For the analysis presented here, the climatological monthly means of these experiments are compared.

Except for orography, the model's boundary conditions are identical in all three experiments. SST boundary conditions are derived from climatological monthly means of the Reynolds reconstructed dataset for the period 1950–92. Sea ice is prescribed according to Rayner et al. (1995), while albedo, ground wetness, and roughness length are prescribed according to Dorman and Sellers (1989). Daily values of the monthly means in the boundary conditions are obtained by linear interpolation in time.

3. Sensitivity of Peruvian stratocumulus to the removal of South American orography

a. Circulation changes in the lower troposphere above the PBL

We first compare the annual cycle of stratocumulus incidence in CTRL and NSAO. Our focus is on the region 20°–10°S, 90°–80°W, where cloud decks are persistent in both observations and CTRL. (We refer to the above domain as the Peruvian stratocumulus region.) The results (Fig. 2a) show that NSAO produces significantly lower area-averaged incidence in the Peruvian stratocumulus region. These results are qualitatively similar to the ones Richter and Mechoso (2004) found for the case of African orography and Namibian stratocumulus. The difference between CTRL and NSAO builds up gradually starting from April and reaches a maximum of approximately 35% in July.

Figure 2b shows the annual cycle of LCS (see section 2 for definition) averaged over the Peruvian stratocumulus region. LCS is higher in CTRL than in NSAO and the difference closely tracks the difference in the annual cycle of stratocumulus incidence. The exception to this is the period from October to December when LCS is almost the same in the two experiments while stratocumulus incidence is still slightly—but not statistically significantly—higher in CTRL (see below in this section).

We further examine LCS by computing its component terms from the simulation results. According to Eq. (2) LCS consists of two terms that involve moist static energy (Δh) and total water mixing ratio (Δr). Analysis of these two terms shows that in both experiments Δh is approximately one order of magnitude larger than Δr. LCS is therefore dominated by the former term. Also, Δh can be further separated into a dry static energy component (Δs) and a water vapor mixing ratio component (Δq). Examining these two contributions we find the former to be dominant so that differences between the two experiments are ultimately dominated by differences in dry static stability between the lowest two model layers.

Let us now examine LTS, which is defined in this paper as the potential temperature difference between 700 mb and the surface. Figure 2c shows that LTS is higher in CTRL than in NSAO during most of the year. Furthermore, the difference in LTS shows a high positive correlation with the concurrent difference in stratocumulus incidence (Fig. 2a). Both start to increase around March and the maximum difference in LTS coincides with the maximum stratocumulus difference. The low value of LTS in NSAO is mostly due to changes at the upper level, as can be seen by comparing the annual temperature cycles at 700 mb and the surface (Figs. 2d and 2e). (Inspection of the terms involved in CTEI yields the same results.) Differences in surface air temperature do not exceed 1 K at any time. This is at least partly due to the constraint placed on surface air temperatures by the prescribed SSTs. In the case of African orography (Richter and Mechoso 2004), however, surface air temperature differences in the Namibian stratocumulus region reached up to 2 K, indicating that there is a potential for greater differences in surface air temperature despite the prescribed SSTs.

We have also tested the statistical significance of the differences in stratocumulus incidence and stability. Figure 2a shows the standard deviation of stratocumulus incidence for each month based on the 20 years and 10 years of simulation in CTRL and NSAO, respectively. Visual inspection of Fig. 2a reveals that the differences between CTRL and NSAO are larger than one standard deviation from May to October. More quantitatively, a Student's t test shows a 99% significance of the differences during all months except February and March. For LCS, the same test suggests significance at the 99% level from April to September. Differences in LTS are significant from March to December, which is largely due to the differences at the upper level. Thus all of the statistical tests indicate high significance of our results for the period April to September. Even though the integrations are comparatively short, the prescribed climatological SSTs limit the amount of interannual variation and allow for high significance of the results.

To gain more insight into the temperature differences between the two experiments, we examine the thermodynamic budget in the Peruvian stratocumulus region. For this analysis we choose the 850-mb level since it is generally close to (though usually above) the center of the second model layer (since the model uses sigma coordinates, the height of the layers is not fixed with respect to pressure). In pressure coordinates, the thermodynamic budget can be written in the form

$$\frac{\partial T}{\partial t} = \frac{\overline{Q}}{c_p} - \left(\frac{p}{p_0}\right)^{\kappa} \omega \frac{\partial \overline{\theta}}{\partial p} - \mathbf{v}\boldsymbol{\nabla}_p \overline{T} - \left(\frac{p}{p_0}\right)^{\kappa} \frac{\partial}{\partial p}(\omega' \theta') - \boldsymbol{\nabla}_p(\mathbf{v}' T'), \tag{6}$$

where T is temperature, t is time, Q is diabatic heating, c_p is the specific heat of dry air at constant pressure, p_0 is a constant reference pressure, $\kappa = R/c_p$, R is the gas constant for dry air, $\omega = Dp/Dt$ is vertical p velocity, $\theta = (p/p_0)^{-\kappa} T$ is potential temperature, and $\mathbf{v}$ is horizontal velocity. Overbars denote monthly means, while primes denote the departure from monthly means. The

left-hand side of Eq. (6) represents the temperature tendency, while the five terms on the right-hand side represent the contributions from diabatic heating, mean vertical temperature advection, mean horizontal temperature advection, vertical temperature advection by transients, and horizontal advection by transients. The annual cycle of these terms is shown in Fig. 3. Diabatic heating in April and May (the months when the difference in stratocumulus incidence starts to increase) is almost identical in the two experiments, but slightly lower in CTRL. The contribution to warming from vertical advection is stronger in CTRL than in NSAO, starting from April and remains so for the rest of the year. Horizontal advection, on the other hand, contributes to cooling in CTRL and to warming in NSAO most of the year. Thus the balance shifts to a stronger positive contribution from vertical advection when mountains are present.

The contribution from transient horizontal advection shown in Fig. 3d is approximately one order of magnitude smaller than the first three terms. Vertical advection by transients (not shown) is another two orders of magnitude smaller. Thus advection by transients does not play an important role in the Peruvian stratocumulus region in the simulation, which is to be expected in the subtropics.

While differences in diabatic heating are small in April and May, they are considerable during other months. This is mostly due to the radiative impact of clouds. In January, the column-integrated cloud amount is higher in CTRL, which leads to less longwave cooling. In July, on the other hand, the free troposphere in CTRL is almost cloud-free, while the PBL is topped by a thick cloud layer. Together with the upward reflected shortwave radiation in CTRL this results in intense radiative cooling above the PBL.

We examine the large-scale circulation changes that accompany the shift in the thermodynamic budget. Our focus is on July, when the differences in stratocumulus incidence between the two experiments are largest. Horizontal velocity and temperature at 850 mb for CTRL and NSAO are shown in Figs. 4a and 4b, respectively.

The blocking effect of the Andes is evident in CTRL (Fig. 4a): easterlies between 20° and 10°S are deflected poleward on the eastern flank, while westerlies around 30°S are deflected equatorward on the western flank. NSAO (Fig. 4b), in comparison, features a far more zonal flow pattern over the whole latitude range shown. Thus the equatorward flow along the South American west coast in CTRL is almost absent in NSAO. Under the assumption that the equatorward flow is predominantly adiabatic, this motion implies sinking of air parcels as they descend along the sloping isentropes (Rodwell and Hoskins 2001). This suggests subsidence strengthening in CTRL compared to NSAO. Stronger subsidence, on the other hand, implies warming through increased vertical temperature advection.

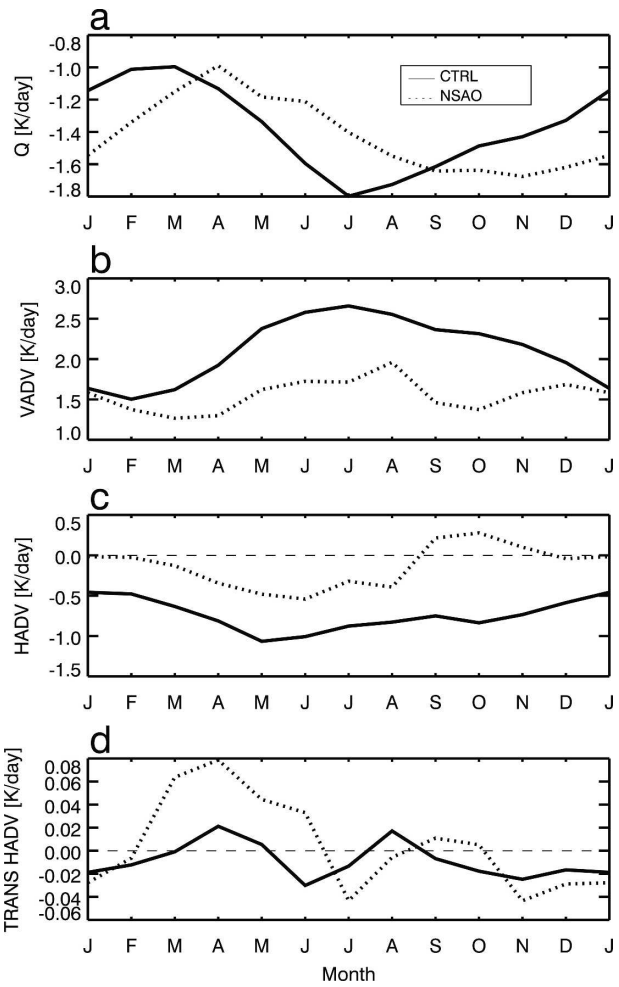

FIG. 3. Annual cycle of terms in the thermodynamic budget at 850 mb averaged over the Peruvian stratocumulus region as defined in the text: (a) diabatic heating (K day^{-1}), (b) vertical temperature advection (K day^{-1}), (c) mean horizontal temperature advection (K day^{-1}), and (d) transient horizontal temperature advection (K day^{-1}). The solid and dotted lines denote CTRL and NSAO, respectively.

The increased LTS can also be explained within the framework of potential vorticity conservation. As the midlatitude westerlies are deflected equatorward, planetary vorticity decreases. Since changes in relative vorticity are comparatively small, the resulting decrease in absolute vorticity has to be balanced by a decrease in column height. Thus the equatorward moving air compresses, which leads to a sharper potential temperature gradient and increased LTS.

Inspection of the vertical pressure velocity (Fig. 5)

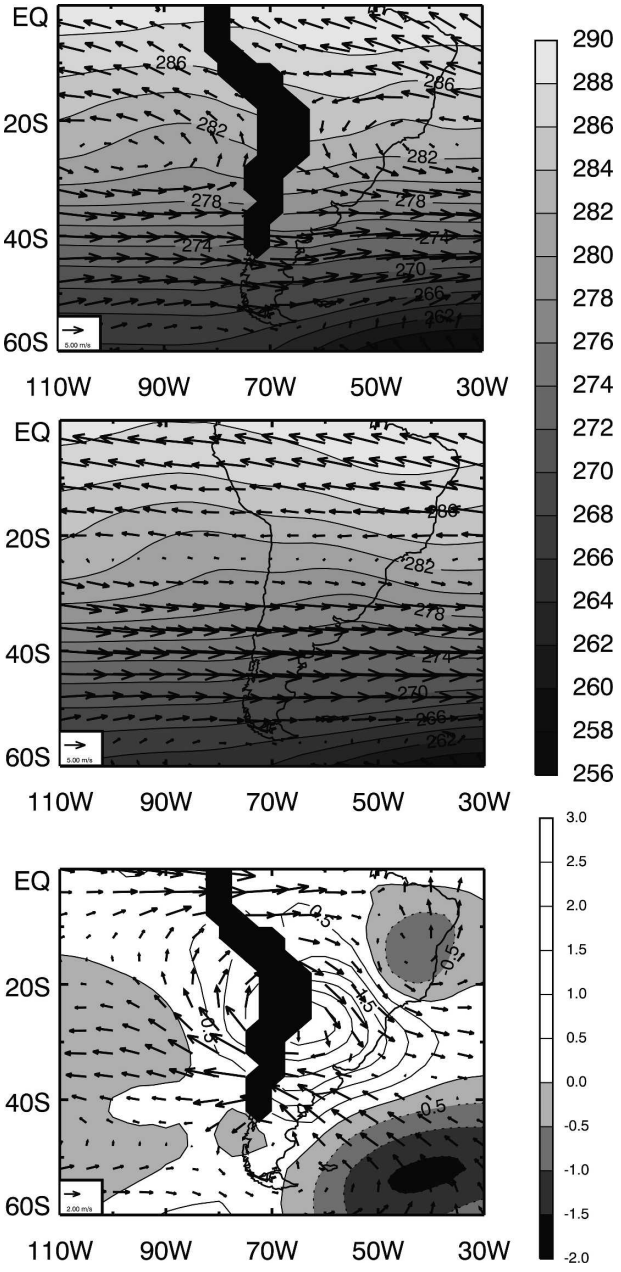

FIG. 4. Wind and temperature at 850 mb in July for (a) CTRL, (b) NSAO, and (c) the difference CTRL minus NSAO. Contour intervals indicate temperature, while arrows indicate horizontal velocity. The reference arrow in the lower left corner corresponds to 5 m s^{-1} in (a) and (b), and 2 m s^{-1} in (c). The blacked out area indicates where orography intersects the 850-mb level.

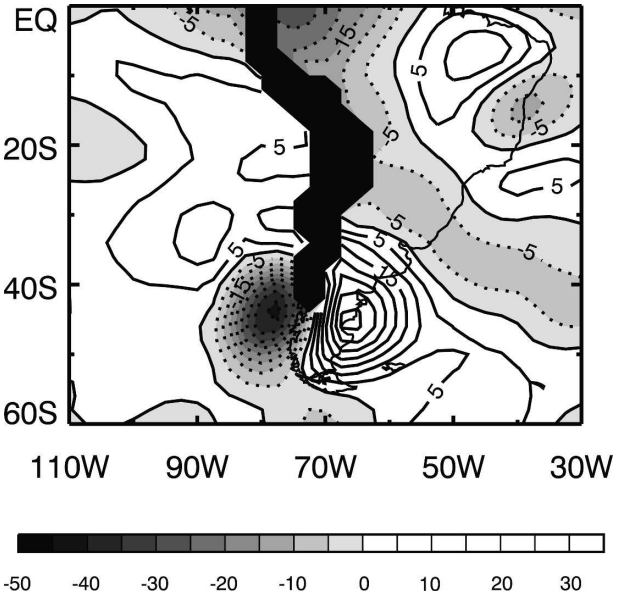

FIG. 5. Difference in vertical p velocity (mb day^{-1}) between CTRL and NSAO for July at 850 mb. Negative values denote stronger upward motion in CTRL, and vice versa. The blacked out area indicates where orography intersects the 850-mb surface.

confirms the stronger subsidence in CTRL west of the Andes and equatorward of 40°S. South of this latitude, on the other hand, there is a dipole pattern in vertical velocity with rising motion to the west of the mountains and sinking motion to the east. A comparison with the patterns of horizontal velocity (Fig. 4) shows that the westerlies at those latitudes tend to pass over the orography rather than being deflected equatorward. The dipole pattern therefore appears to be a consequence of the orographic forcing, namely rising motion on the upslope and sinking motion on the downslope. Thus the following picture emerges: as midlatitude westerlies approach the western flank of the Andes, they become subject to orographic uplift that increases their potential energy. Part of the flow ascends high enough to pass the orographic barrier, while the remaining part is deflected equatorward and in the process sinks along the sloping isentropes. This is associated with subsidence, and hence warming by vertical temperature advection.

We seek further confirmation of the process described above by examining air parcel trajectories. A total count of 100 air parcels are released in a rectangular area ranging from 40° to 4°S, 100° to 55°W, which is southeast and hence upstream of the Peruvian stratocumulus region. Inside the area, the parcels are initially placed on a regular mesh with 10 points in both the longitudinal and latitudinal direction. Since our interest is in the process of equatorward deflection and subsequent sinking of the flow, we examine parcels released at 1500 m, which is low enough for blocking to be effective and high enough to allow for sinking above the stratocumulus region.

In July, air parcel trajectories in CTRL and NSAO show significant differences (Fig. 6a). In CTRL, most

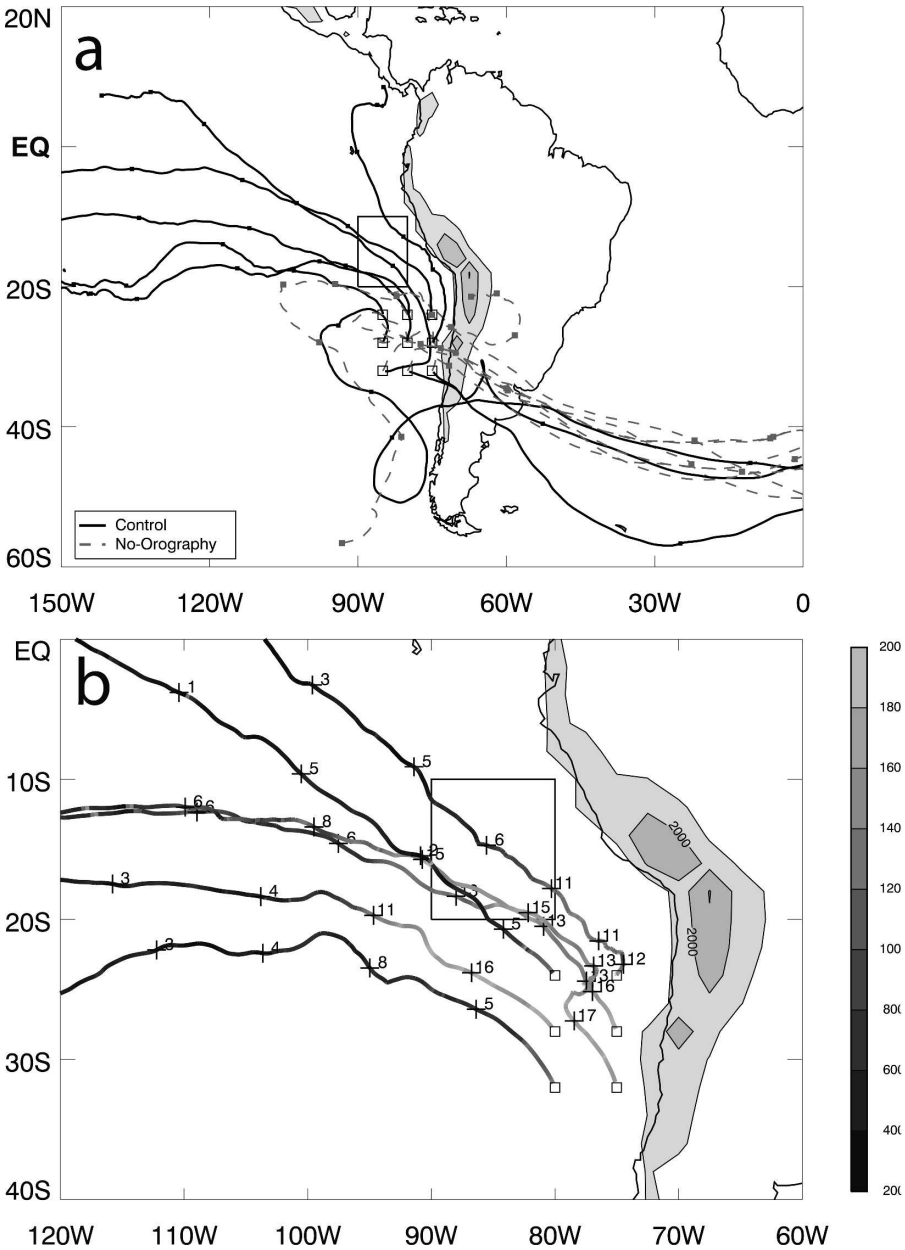

FIG. 6. (a) Air parcel trajectories for parcels released at 1500 m on 23 June. The trajectories show 15 days, with solid squares indicating 3-day intervals. CTRL and NSAO are denoted by blue and red lines, respectively. The contour lines represent the orography used in CTRL, with a contour interval of 1000 m. The open squares to the west of South America indicate the initial positions of the parcels. (b) As in (a) but for trajectories in CTRL only. The trajectories are annotated with air parcel height (in 100 m) at 2-day intervals (marked by crosses). Air parcel height is also indicated by the gray shading of the trajectories.

trajectories curve equatorward and do not cross the orographic barrier. In NSAO, on the other hand, most trajectories cross the South American continent, thus confirming the circulation patterns in the Eulerian fields (Fig. 4). These results are consistent with the notion that orography deflects the low-level flow equatorward. Figure 6b illustrates the downward motion of the air parcels as they move equatorward. Thus the trajectories provide a good illustration of the scenario that we suggested for the Peruvian stratocumulus region and its vicinity.

In January, trajectories in both CTRL and NSAO

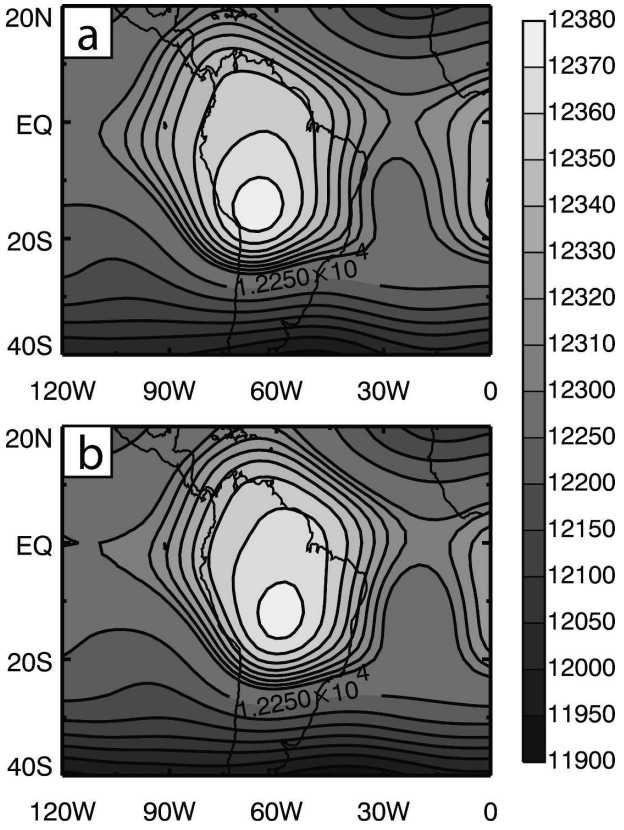

FIG. 7. Geopotential height (m) at the 200-mb level in January for (a) CTRL and (b) NSAO.

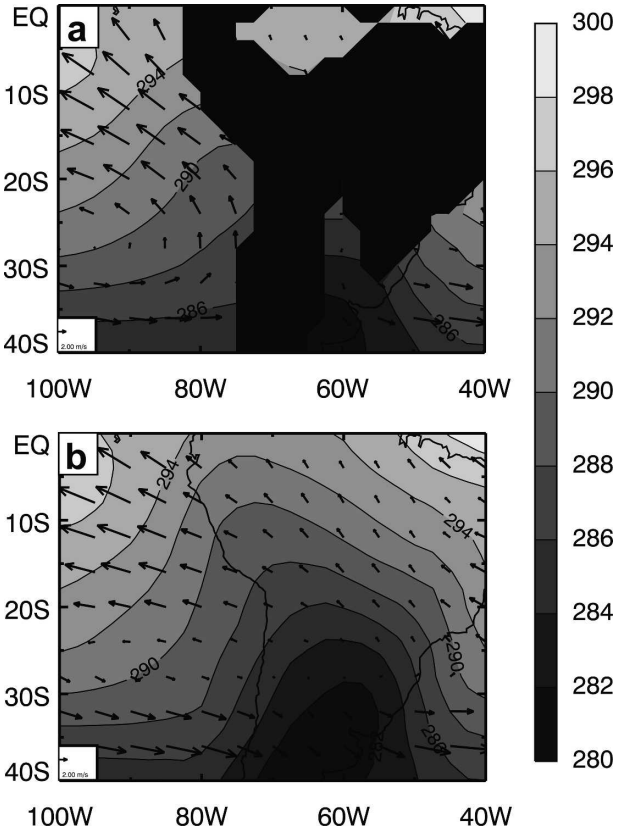

FIG. 8. July wind (m s^{-1}) and temperature (K) at 1000 mb for (a) CTRL and (b) NSAO. The reference arrow in the lower left corner of each panel indicates a wind speed of 2 m s^{-1}.

predominantly curve equatorward along the South American coast rather than crossing the continent (not shown). The fact that parcels move equatorward even when orography is absent is consistent with the strong anticyclonic circulation over the southern Pacific. The position and strength of the anticyclone depends on many factors, and is topic of ongoing research (e.g., Seager et al. 2003). Two factors that must play an important role are the land–sea contrast during summertime and Rossby wave subsidence induced by convection associated with the South American monsoon system (Rodwell and Hoskins 2001). The latter forms a major feature of the summer circulation over South America. CTRL produces a fairly realistic representation of the South American monsoon system, as evidenced by the patterns of vertical and horizontal velocity (not shown) and the patterns of geopotential height at 200 mb (Fig. 7a). The Bolivian high in CTRL compares favorably with NASA Data Assimilation Office (NASA/DAO) data [as presented, e.g., in Lenters and Cook (1997), their Fig. 2a] but places the center of the high a little farther west toward the Andes.

Inspection of the geopotential height in NSAO (Fig. 7b) indicates that the monsoonal circulation is well captured in that simulation as well. This agrees with the results of Lenters and Cook (1997), who also found a realistic simulation of the South American monsoon system in a GCM experiment without South American orography.

b. Circulation and moisture changes inside the PBL

To examine the influence of surface processes on stratocumulus incidence we start by comparing patterns of surface flow and air temperature in CTRL and NSAO for July (Fig. 8). The orography blocks and deflects flow at this level, which is manifested in the stronger equatorward flow in CTRL. This pattern prevails throughout the year (not shown) but is strongest during winter. As seen at the 850-mb level (section 3a), the blocking effect of orography is most evident in July (local winter), when the land–sea contrast between the southeastern subtropical Pacific and South America is weakest. This illustrates how orographic forcing plays an important role in closing off the Pacific anticyclone over the ocean during that part of the year. In the ab-

sence of orography the flow is predominantly zonal (Fig. 8b). The sea level pressure fields (Fig. 9) confirm that during July the Pacific subtropical high is much more localized over the ocean when orography is present.

Surface air temperatures over the southeastern Pacific are approximately 0.5 K lower in CTRL than in NSAO (not shown). Thus, even though the differences in surface flow between CTRL and NSAO are substantial, there are no similarly significant differences in surface air temperature in the Peruvian stratocumulus region. This is due, in part, to the use of identical SST distributions in the two experiments. However, the orientation of wind and temperature gradients plays a role in this too. The July surface winds in CTRL are equatorward and along the west of the continent (Fig. 8a), which implies cold air advection into the Peruvian stratocumulus region. In NSAO, on the other hand, the surface flow toward the Peruvian stratocumulus region is from the continent, which also implies cold air advection due to the low ground temperatures during winter. To quantify this, we calculated the horizontal temperature advection at the surface level. The results indicate that advective cooling is indeed quite similar in CTRL and NSAO, with a tendency for stronger cooling in the former experiment.

The coldest surface air temperatures in CTRL, relative to NSAO, occur in October. This is likely due to warm air advection from the continent in the latter experiment. The differences, however, are highly confined to the coastal region, and do not affect the Peruvian stratocumulus region greatly.

To summarize the orographic impact on the low-level temperature field, we find that, in CTRL, blocking and equatorward deflection of the surface flow lead to stronger cold air advection than in NSAO. Consistently, surface air temperatures over the southeastern Pacific are colder in CTRL, but the prescribed SSTs mitigate this effect. Thus, the difference in surface air temperatures is small and increases only by a small amount the stability in CTRL compared to the one in NSAO.

We next examine the moisture differences in the PBL between the two experiments. Figure 10a shows that from January to April and from October to December PBL specific humidity is lower in CTRL than in NSAO (from May to September it is approximately the same in the two experiments). This behavior of PBL specific humidity does not contradict the higher stratocumulus incidence in CTRL. Even though specific humidity is lower in CTRL, the PBL in that experiment is much deeper during most of the year (Fig. 10b).

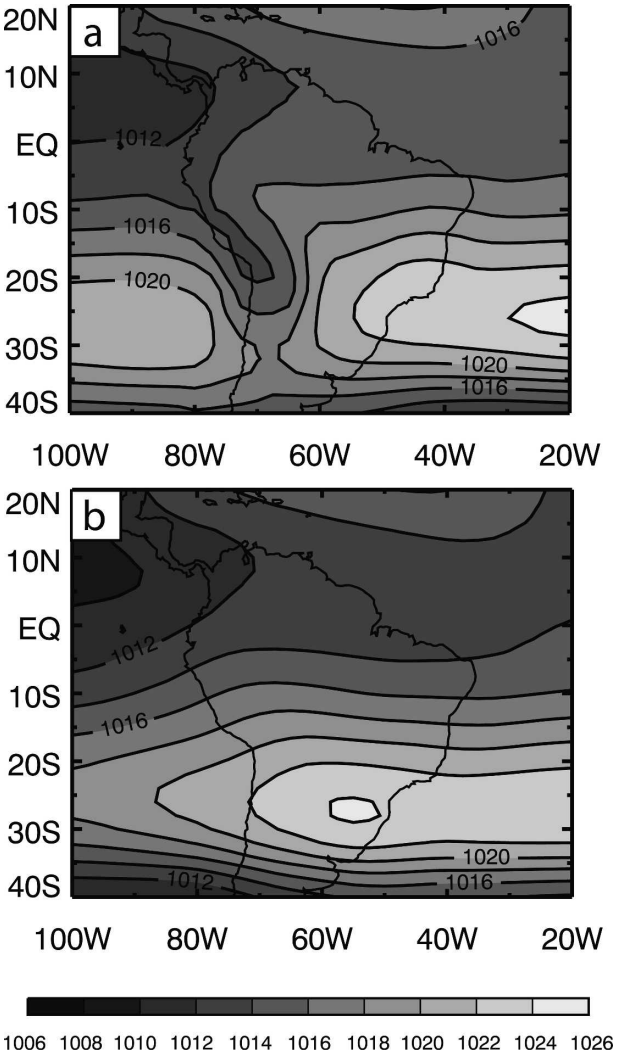

FIG. 9. Sea level pressure (mb) in July for (a) CTRL and (b) NSAO.

Therefore, saturation is achieved more readily in CTRL since the PBL top is higher and the average PBL temperature colder.

From a different perspective, one could argue that, because the PBL in CTRL is thicker, its total moisture content can be higher even when specific humidity is lower than in NSAO. To examine whether this is the case in the Peruvian stratocumulus region, we calculate the PBL moisture content by multiplying PBL depth (which is a measure of its mass) with total water mixing ratio and the total horizontal area of the Peruvian stratocumulus region. The results in Fig. 10c confirm that PBL moisture content is higher in CTRL throughout the year. Consistent with the increased PBL moisture content in CTRL, surface evaporation (Fig. 10d) is also higher in that experiment throughout the year. The in-

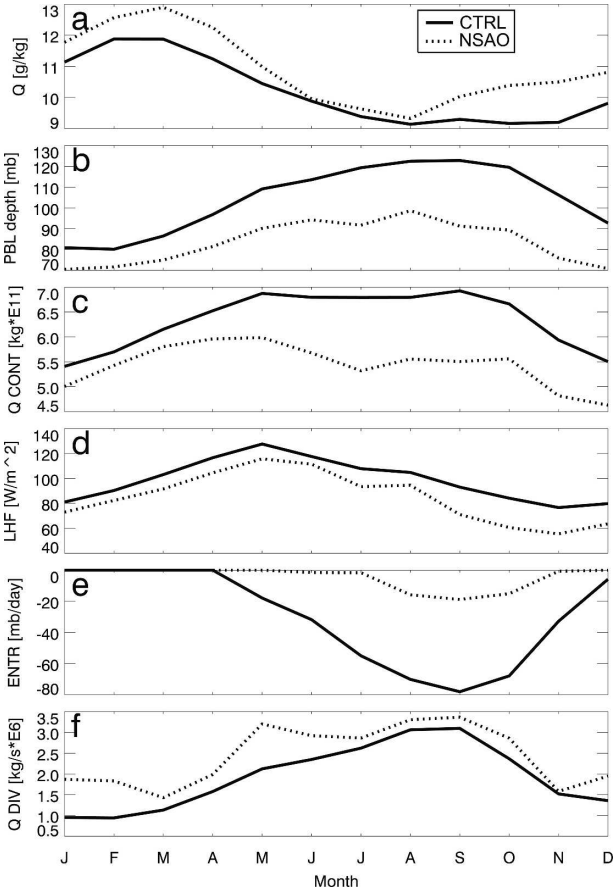

FIG. 10. Annual cycle of terms related to the PBL moisture budget. All terms are averaged over the Peruvian stratocumulus region as defined in the text. Shown are (a) specific humidity (g kg^{-1}), (b) PBL depth (mb), (c) PBL moisture content (kg $\times$ 10^{11}), (d) surface evaporation (kg $s^{-1} \times 10^6$), (e) entrainment drying (kg $s^{-1} \times 10^6$), and (f) PBL moisture flux divergence (kg $s^{-1} \times 10^6$). The solid and dashed lines denote CTRL and NSAO, respectively.

creased surface evaporation, in turn, can be seen as a response to the increased drying from PBL top entrainment (Fig. 10e).

The horizontal PBL moisture flux divergence in the region (Fig. 10f) is slightly higher in NSAO than in CTRL most of the year, which, at least in part, reflects the intrusion of dry continental air in the absence of orography. This assists in keeping the PBL moisture content higher in CTRL than in NSAO.

In the above considerations of the PBL moisture budget we have neglected the contribution from the PBL cumulus mass flux. This process can remove substantial amounts of water vapor from the PBL. In the region of interest, however, cumulus activity is very weak in both experiments and has not been included in Fig. 10.

4. Comparison with the African case

Similar to the African case (Richter and Mechoso 2004), we found that stratocumulus to the west of South America are significantly reduced in the absence of orography and that the strongest impact occurs during local winter. In contrast to the African case, however, the difference in stratocumulus incidence starts to develop earlier, in local fall, when incidence gradually increases in CTRL but almost remains unchanged in NSAO.

At the surface level the circulation changes induced by orography are very similar to the African case: as the midlatitude westerlies impinge on the Andes they are partially deflected equatorward, which is associated with cold air advection. In both cases the absence of cold air advection in the no-orography experiments (NSAO and No-African-Orography experiment) has an only moderate impact on surface air temperatures.

Above the PBL, on the other hand, there is a fundamental difference between the orographic impact in the Peruvian and Namibian stratocumulus regions as a consequence of the height differences between the mountains of Africa and South America. The orography of South America is high enough to cause substantial blocking of the lower tropospheric flow. This leads to mostly poleward deflection of the trade easterlies on the eastern flank of the Andes, and equatorward deflection of the midlatitude westerlies on their western flank. The Peruvian stratocumulus region is then influenced by the equatorward deflected flow. Around the 850-mb level, this flow is approximately along the equatorward sloping isentropes, thereby enhancing subsidence over the Peruvian stratocumulus region. Within the PBL, on the other hand, the flow is equatorward along the ocean surface and advects cold midlatitude air toward the Peruvian stratocumulus region. Both of these effects combine to increase LTS in the region and provide an environment conducive to the development and persistence of stratocumulus.

The African case presents a different picture (see Richter and Mechoso 2004). Here orographic heights are not sufficient to cause blocking of the flow. As a result, trade easterlies from the Indian Ocean are able to cross southern Africa down to a height of about 800 mb. Consistent with conservation of potential vorticity, this results in an anticyclonic circulation centered over the continent at around 700 mb. Part of this flow pattern extends over the Atlantic Ocean off the coast of Namibia where it leads to warm horizontal advection at 700 mb and increased stability of the lower troposphere, as evidenced by an analysis of the thermodynamic energy budget.

Since the South American continent and its associated orography extend farther poleward than Africa, there clearly is a potential for stronger interaction with the midlatitude westerlies. Our results suggest that this potential is realized.

Thus the mechanisms by which LTS is increased are fundamentally different in the two regions. In the case of South America, it is compression of equatorward deflected air that causes a sharpening of the lower tropospheric temperature gradient and LTS. In the case of Africa, on the other hand, it is poleward advection of warm air above the PBL that is mostly responsible for the high values of LTS in the stratus region. The fundamental difference between the two regions is also evident in the lower-tropospheric flow patterns. In the South American case air both within and above the PBL is moving equatorward, while in the African case the flow is equatorward within the PBL but poleward above.

In both the African and the South American cases the basic seasonal cycle of stratocumulus was preserved, even in the absence of orography. Therefore, it seems that the underlying SSTs are still the dominant factor in generating the seasonal cycle of stratocumulus incidence. Since SSTs are prescribed in our model, we do not take into account the feedbacks that could arise in the coupled ocean–atmosphere system.

5. Sensitivity of Peruvian stratocumulus to smoothing of South American orography

The representation of orography in GCMs is, by necessity, an idealization of the real world. Modern satellite techniques have enabled us to obtain topographic datasets at resolutions of 1 km by 1 km and beyond. Such detailed orography cannot be incorporated directly into current general circulation models, which employ grid sizes on the order of 100 km. To assign surface elevations to model grid points, some type of averaging is usually applied to the high-resolution data. In the preparation of the orographic boundary conditions used in versions of our model, for example, we take the average of all high-resolution data points that fall into a given grid cell and then assign the average to that grid cell. This results in implicit smoothing of the high-resolution dataset, where the term implicit indicates that it is an inevitable consequence of representing high-resolution data on a GCM grid in a meaningful way. Additional explicit smoothing is often performed in order to avoid computational difficulties in regions of steep and high orography, such as the Andes and Antarctica. In the case of our model, the smoothing applied to the Andes reduces their maximum height by about 1000 m (Fig. 11).

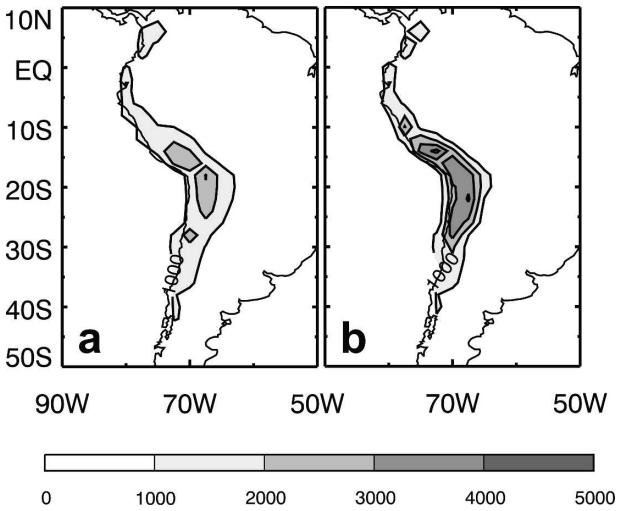

FIG. 11. Orographic boundary conditions (m) in CTRL and USAO. Contour interval is 1000 mb.

We saw that orographic effects significantly increase the amount of simulated stratocumulus over the oceanic regions to the west (see section 3, and also Richter and Mechoso 2004). This raises the question whether a more realistic representation of orography could have a significant impact on stratocumulus and whether this impact might be beneficial to the simulation of the subtropical climate system.

To test the sensitivity of Peruvian stratocumulus to the representation of orography we performed a 5-yr integration in which no smoothing was applied to the orography of South America. We will refer to this experiment as USAO (unsmoothed South American orography). Results from the sensitivity experiment are then compared with the same control experiment used in section 3. The orographic boundary conditions in the two experiments are contrasted in Figs. 11a and 11b, which show that in USAO a comparatively large area exceeds 3000 m and a few peaks exceed 4000 m. The corresponding features in CTRL are about 1000 m lower.

Despite the considerable differences in orographic height between the two experiments, there are no significant changes in stratocumulus incidence in the Peruvian stratocumulus region (Fig. 12a). Only September features an appreciable difference, with higher incidence in CTRL than in USAO. The value of LCS [Eq. (1), Fig. 12b] is very similar in the two experiments, which is also reflected in the annual cycle of LTS (not shown).

These results suggest that, in the context of a GCM, a more realistic representation of the orography of South America does not lead to significantly higher

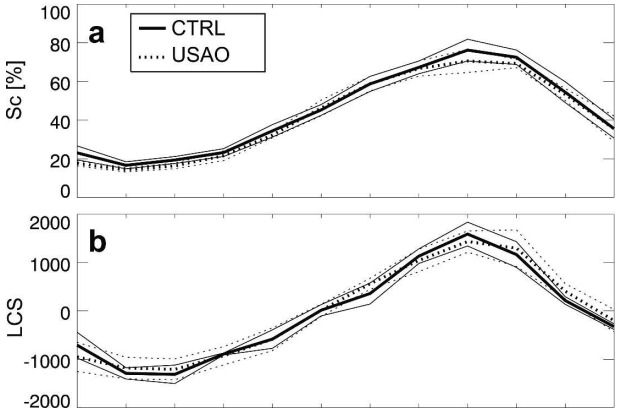

FIG. 12. Annual cycle of (a) stratocumulus incidence (%) and (b) LCS. Both variables are averaged over the Peruvian stratocumulus region. The thick solid and dashed lines denote CTRL and USAO, respectively, while the thin solid and dashed lines show the standard deviation interval for individual months.

stratocumulus incidence in the Peruvian stratocumulus region. This conflicts with the results of Xu et al. (2004), who report a significant decrease in low-level cloud fraction when a smoothed GCM orography is employed in their regional atmospheric model.

Although there are many differences between the regional model of Xu et al. and our AGCM, probably the most fundamental one lies in the treatment of the PBL. Our model is based on a mixed-layer representation of the PBL. The regional model attempts to explicitly resolve the PBL vertical structure with its 10 model levels below 800 mb (compared to 2–3 layers below 800 mb in our model). The impression of a much higher resolution in the regional model can be deceptive, however. While in the AGCM the jump across the PBL top is explicitly represented, it has to be resolved in the regional model. In the subtropical stratocumulus regions this jump tends to be rather sharp and the ten layers in the regional model will not suffice to resolve it. It should also be noted that Xu et al. discuss their results in terms of column-integrated liquid water content, which may not be representative of PBL cloud incidence.

6. Summary and discussion

We have examined the impact of South American orography on the persistence and annual cycle of Peruvian stratocumulus clouds. This was done by comparing a 20-yr control simulation with a 10-yr simulation in which South American orography was removed.

In the absence of orography, stratocumulus incidence off the Peruvian coast is significantly reduced, with the greatest impact during austral winter. LTS in the two experiments shows a similar seasonal cycle in the region, with reduced values in NSAO for roughly the same period that stratocumulus incidence is reduced. Thus there is a high positive correlation between stratocumulus incidence and LTS in the Peruvian stratocumulus region. The higher LTS in CTRL is largely the result of higher temperatures at 850 mb, with a smaller contribution from the surface level.

Inspection of the terms relevant to the CTEI mechanism confirms that dry static stability (and thus LTS) is crucial to the higher stratocumulus incidence in CTRL. This motivated us to further investigate how orography brings about higher LTS in CTRL.

Within the PBL, midlatitude westerlies impinging on the Andes are partially deflected equatorward. This leads to cold air advection at the surface, but the effect is mitigated by the prescribed SSTs so that the resulting cooling of surface air temperatures is only small to moderate.

In the lower troposphere above the PBL, there is stronger subsidence when South American orography is present. The stronger subsidence in CTRL is associated with stronger vertical temperature advection, and thus contributes positively to the warmer temperatures above the PBL and increased LTS. Analysis of the thermodynamic budget over the Peruvian stratocumulus region shows that, starting from April, vertical advection is the only process contributing positively to the higher temperatures in CTRL. Horizontal advection, on the other hand, is close to zero or negative throughout the year in CTRL.

The reason why subsidence and vertical advection are stronger in CTRL seems to lie in the equatorward deflection of westerly flow by the orography. At upper levels this leads to sinking motion as the flow descends on the sloping isentropes. In NSAO, conversely, deflection by orography does not occur and, accordingly, equatorward winds are much reduced most of the year. Only during local summer is there significant equatorward flow in NSAO, which appears to be a consequence of the monsoonal flow patterns during that part of the year. Consistently, temperatures in the lower troposphere above the PBL are warmer in CTRL from March to November, but not from December to February. Further confirmation for the sinking along isentropes comes from our analysis of air parcel trajectories.

We saw, in section 3b, that the PBL is deeper in CTRL than in NSAO and that this allows for a higher PBL moisture content in CTRL, even though specific humidity is lower there than in NSAO. At the same time, a deeper PBL implies that saturation is achieved

more easily at the top of the layer. Part of the reason why the PBL is deeper in CTRL is that PBL-top entrainment is larger in that experiment. PBL-top entrainment in the UCLA AGCM is intimately linked to stratocumulus incidence such that entrainment will be enhanced significantly due to cloud-top radiative forcing when stratocumulus is present. Thus there exists a positive feedback loop among stratocumulus incidence, entrainment, and PBL depth, which makes it more difficult to identify a single reason for the higher stratocumulus incidence in CTRL. Our argument is that the high value of LCS in CTRL would exist even in a completely dry atmosphere since equatorward deflection and sinking along isentropes do not rely on the presence of moisture. A high value of LCS, on the other hand, allows for high incidence of stratocumulus. Entrainment and PBL depth then increase as a consequence of the high stratocumulus incidence. Thus we believe that the initial reason for the higher stratocumulus incidence in CTRL lies in the higher stability in that experiment. We conclude that the South American orography interacts with the atmospheric circulation in a way to achieve higher stability in the lower troposphere. This allows stratocumulus to become more prevalent, which in turn engenders a higher entrainment rate and PBL growth. The associated drying effect is counteracted by an increase in latent heat flux such that specific humidity in CTRL and NSAO is almost the same.

In the present study we have not addressed the potential impact of coupled ocean–atmosphere feedbacks in modifying the orographic response. Kitoh (2004) conducted no-orography experiments with both an AGCM and a coupled ocean–atmosphere GCM. His results suggest that coupling intensifies the orographic response over the subtropical regions (i.e., stronger anticyclones, more low-level cloud) but does not alter it qualitatively. Our uncoupled results indicate a strengthening of the surface wind stress over the Peruvian stratus region from May to September (Fig. 13c) when orography is present. Furthermore latent heat flux into the atmosphere is stronger in CTRL year round (Fig. 13b), while the shortwave flux into the ocean is consistently lower (Fig. 13d). As a result, the uptake of energy by the ocean is less in CTRL than in NSAO yearround (Fig. 13f). This suggests that the orographic impact in our AGCM would intensify in a coupled scenario.

A caveat to the findings of Kitoh (2002, 2004) is that his coupled GCM uses a flux correction scheme that is designed to produce climatological SSTs, thereby limiting the ability of the oceanic component to evolve freely. We are therefore currently working on a coupled ocean–atmosphere model that will allow us to validate our results.

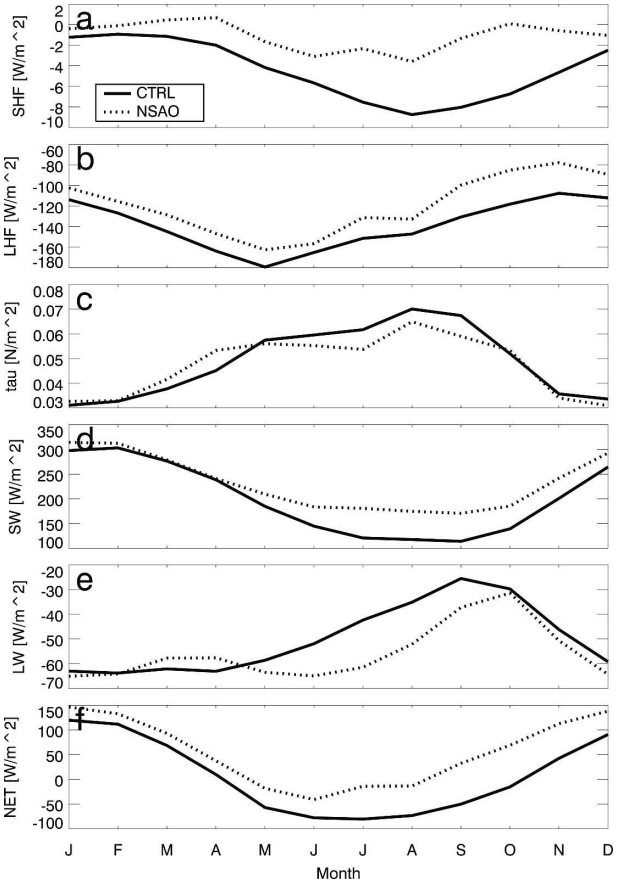

FIG. 13. Annual cycle of surface fluxes (downward positive) over the Peruvian stratus region. Fluxes of (a) sensible heat (W m^{-2}), (b) latent heat (W m^{-2}), (c) momentum (N m^{-2}), (d) net longwave (W m^{-2}), (e) net shortwave (W m^{-2}), and (f) net energy (W m^{-2}).

In our study, we have focused on subtropical stratocumulus in the Southern Hemisphere. There are also two major stratus regions in the Northern Hemisphere, one off the coast of northwest Africa, the other off the coast of California (Klein and Hartmann 1993). In both these regions, stratocumulus incidence peaks in local summer when the underlying SSTs are well above their annual minumum while land–sea contrasts are at a maximum. This suggests that circulation patterns associated with the North American and North African monsoons (which are also affected by orography) are dominant in the seasonal cycle of the Northern Hemisphere stratocumulus. Additionally, the Californian and Canarian stratus regions are located farther poleward than their Southern Hemisphere counterparts and are thus more susceptible to the influence of midlatitude disturbances. Because of these differences, it is

difficult to extrapolate to the Northern Hemisphere the results presented in this study, which emphasizes the dynamical effects of orography.

7. Conclusions

In the introduction we identified three questions to be addressed in the present study. Our conclusions are organized according to these questions:

1) *What is the impact of South American orography on Peruvian stratocumulus?* South American orography contributes significantly to create conditions favorable to the development of high stratocumulus incidence in the Peruvian stratocumulus region, with the greatest impact occurring in austral winter. This has been interpreted in the context of the increase in lower-tropospheric stability and decrease in the incidence of cloud-top entrainment instability. This gives further credence to our results with respect to the real world, because observational studies have shown a close link between stratocumulus incidence and LTS.

The circulation changes in the lower troposphere are consistent with this scenario. As midlatitude westerlies approach the South American continent they are blocked and deflected equatorward. Above the PBL, this results in subsiding motion as the air moves along sloping isentropes. Thus subsidence over the Peruvian stratocumulus region is stronger when mountains are present and this is associated with stronger subsidence warming. Inside the PBL, the equatorward deflected flow moves parallel to the surface and advects cold air toward the Peruvian stratocumulus region. This effect, however, is damped by the prescribed SSTs, and therefore the larger contribution to high stability stems from the flow pattern above the PBL.

2) *How does the orographic impact on Peruvian stratocumulus differ from the case of southern Africa?* Even though enhanced stability occurs in both stratocumulus regions when orography is present, the underlying mechanisms are fundamentally different. This appears to be a consequence of the height differences between the mountains of Africa and South America. The steeper and higher mountains of South America do not permit an anticyclonic circulation pattern over the continent as in the case of southern Africa (Richter and Mechoso 2004). Thus the mechanism of horizontal warm air advection is not active in the Peruvian stratocumulus region. Instead, the equatorward deflection of midlatitude westerlies, and their subsequent sinking along isentropes result in warmer temperatures and hence higher LTS above the Peruvian stratocumulus region.

At the surface, on the other hand, the westerly flow is deflected equatorward by orography in both cases. This brings cold air to the Peruvian and Namibian stratocumulus regions, and contributes to an environment that favors high incidence of stratocumulus.

3) *Does smoothing of the South American orography deteriorate the simulation of Peruvian stratocumulus?* Our results do not support this idea. Even though the Andes are, on average, approximately 1000 m higher in USAO than in CTRL, stratocumulus incidence off the Peruvian coast does not show any significant differences between the two experiments. Employing a more realistic mean orography does, therefore, not carry any promise of improving the simulation of stratocumulus in the UCLA AGCM.

In the introduction of this paper we mentioned that selecting an approach based on an AGCM precludes the consideration of ocean atmosphere feedbacks. In view of our results we can speculate that the weakened equatorward flow at the ocean surface along the Peruvian coast in the absence of mountains would significantly weaken coastal upwelling and result in significantly warmer SSTs along the coast of South America than those prescribed in the uncoupled model. Contemporary coupled ocean–atmosphere GCMs, however, have major difficulties in the simulation of coastal upwelling regions. Much more work is required to produce a coupled GCM that will allow for the refinement of our results in a more general context.

Acknowledgments. This study was supported by NOAA under Grant NA04OAR4310095. Model integrations were performed at the NCAR computing facilities. The authors thank Dr. J. D. Farrara for assistance with the model integrations and many helpful discussions. Thanks also to Professor A. Arakawa and Professor B. Stevens for their useful comments on this work.

REFERENCES

Arakawa, A., and W. H. Schubert, 1974: Interaction of a cumulus ensemble with the large-scale environment. Part I. *J. Atmos. Sci.,* **31,** 674–701.

Bretherton, C. S., and M. C. Wyant, 1997: Moisture transport, lower tropospheric stability, and decoupling of cloud-topped boundary layers. *J. Atmos. Sci.,* **54,** 148–167.

Charney, J. G., and A. Eliassen, 1949: A numerical method for predicting the perturbations of the middle latitude westerlies. *Tellus,* **1,** 38–54.

Cheng, M.-D., and A. Arakawa, 1997: Inclusion of rainwater budget and convective downdrafts in the Arakawa–Schubert cumulus parameterization. *J. Atmos. Sci.,* **54,** 1359–1378.

Davey, M. K., and Coauthors, 2002: STOIC: A study of coupled model climatology and variability in tropical ocean regions. *Climate Dyn.,* **18,** 403–420.

Deardorff, J. W., 1972: Parameterization of the planetary bound-

ary layer for use in general circulation models. *Mon. Wea. Rev.,* **100,** 93–106.

Dorman, J. L., and P. J. Sellers, 1989: A global climatology of albedo, roughness length and stomatal resistance for atmospheric general circulation models as represented by the Simple Biosphere Model (SiB). *J. Appl. Meteor.,* **28,** 838–855.

Harshvardhan, R. Davies, D. A. Randall, and T. G. Corsetti, 1987: A fast radiation parameterization for general circulation models. *J. Geophys. Res.,* **92,** 1009–1016.

——, D. A. Randall, T. G. Corsetti, and D. A. Dazlich, 1989: Earth radiation budget and cloudiness simulations with a general circulation model. *J. Atmos. Sci.,* **46,** 1922–1942.

Held, I. M., and M. Ting, 1990: Orographic versus thermal forcing of stationary waves: The importance of the mean low-level wind. *J. Atmos. Sci.,* **47,** 495–500.

Hoskins, B. J., 1996: On the existence and strength of the summer subtropical anticyclones—Bernhard Haurwitz memorial lecture. *Bull. Amer. Meteor. Soc.,* **77,** 1287–1292.

Kitoh, A., 2002: Effects of large-scale mountains on surface climate—A coupled ocean–atmosphere general circulation model study. *J. Meteor. Soc. Japan,* **80,** 1165–1181.

——, 2004: Effects of mountain uplift on East Asian summer climate investigated by a coupled atmosphere–ocean GCM. *J. Climate,* **17,** 783–802.

Klein, S. A., and D. L. Hartmann, 1993: The seasonal cycle of low stratiform clouds. *J. Climate,* **6,** 1587–1606.

——, ——, and J. R. Norris, 1995: On the relationship among low cloud structure, sea surface temperature, and atmospheric circulation in the summertime northeast Pacific. *J. Climate,* **8,** 1140–1155.

Köhler, M., 1999: Explicit prediction of ice clouds in general circulation models. Ph.D. thesis, University of California, Los Angeles, 146 pp.

Lenters, J. D., and K. H. Cook, 1997: On the origin of the Bolivian high and related circulation features of the South American climate. *J. Atmos. Sci.,* **54,** 656–677.

Li, J.-L., A. Aarakawa, and C. R. Mechoso, 1999: Improved simulation of PBL moist processes with the UCLA GCM. Preprints, *Seventh Conf. on Climate Variations*, Long Beach, CA, Amer. Meteor. Soc., 423–426.

——, M. Köhler, J. D. Farrara, and C. R. Mechoso, 2002: The impact of stratocumulus cloud radiative properties on surface heat fluxes simulated with a general circulation model. *Mon. Wea. Rev.,* **130,** 1433–1441.

Lilly, D. K., 1968: Models of cloud-topped mixed layers under a strong inversion. *Quart. J. Roy. Meteor. Soc.,* **94,** 292–309.

Mechoso, C. R., and Coauthors, 1995: The seasonal cycle over the tropical Pacific in coupled ocean–atmosphere general circulation models. *Mon. Wea. Rev.,* **123,** 2825–2838.

Mellor, G. L., T. Ezer, and L.-Y. Oey, 1994: The pressure gradient conundrum of sigma coordinate ocean models. *J. Atmos. Oceanic Technol.,* **11,** 1126–1134.

Pan, D.-M., and D. A. Randall, 1998: A cumulus parameterization with a prognostic closure. *Quart. J. Roy. Meteor. Soc.,* **124,** 949–981.

Randall, D. A., 1980a: Entrainment into a stratocumulus layer with distributed radiative cooling. *J. Atmos. Sci.,* **37,** 148–159.

——, 1980b: Conditional instability of the first kind upside-down. *J. Atmos. Sci.,* **37,** 125–130.

Rayner, N. A., C. K. Folland, D. E. Parker, and E. B. Horton, 1995: A new global sea-ice and sea surface temperature (GISST) data set for 1903–1994 for forcing climate models. Hadley Centre Internal Note 69, U.K. Meteorological Office, 14 pp.

Richter, I., and C. R. Mechoso, 2004: Orographic influences on the annual cycle of Namibian stratocumulus clouds. *Geophys. Res. Lett.,* **31,** L24108, doi:10.1029/2004GL020814.

Ringler, T., and K. H. Cook, 1999: Understanding the seasonality of orographically forced stationary waves: Interaction between mechanical and thermal forcing. *J. Atmos. Sci.,* **56,** 1154–1174.

Rodwell, M. J., and B. J. Hoskins, 2001: Subtropical anticyclones and summer monsoons. *J. Climate,* **14,** 3192–3211.

Rossow, W. B., and R. A. Schiffer, 1991: ISCCP cloud data products. *Bull. Amer. Meteor. Soc.,* **72,** 2–20.

Seager, R., R. Murtugudde, N. Naik, A. Clement, N. Gordon, and J. Miller, 2003: Air–sea interaction and the seasonal cycle of the subtropical anticyclones. *J. Climate,* **16,** 1948–1966.

Stevens, B., 2002: Entrainment in stratocumulus-topped mixed layers. *Quart. J. Roy. Meteor. Soc.,* **128,** 2663–2690.

——, and Coauthors, 2003: On entrainment rates in nocturnal marine stratocumulus. *Quart. J. Roy. Meteor. Soc.,* **129,** 3469–3493.

Suarez, M. J., A. Arakawa, and D. A. Randall, 1983: The parameterization of the planetary boundary layer in the UCLA general circulation model: Formulation and results. *Mon. Wea. Rev.,* **111,** 2224–2243.

Webster, S., A. R. Brown, D. R. Cameron, and C. P. Jones, 2003: Improvements to the representation of orography in the Met Office Unified Model. *Quart. J. Roy. Meteor. Soc.,* **129,** 1989–2010.

Xu, H., Y. Wang, and S. Xie, 2004: Effects of the Andes on eastern Pacific climate: A regional atmospheric model study. *J. Climate,* **17,** 589–602.